

Effect of Binary Fraction on Horizontal Branch Morphology under Tidally Enhanced Stellar Wind

Zhenxin LEI

Department of Science, Shaoyang University, Shaoyang 422000, China

Key Laboratory for the Structure and Evolution of Celestial Objects, Chinese Academy of Sciences, Kunming 650011, China

lzx2008@ynao.ac.cn

Xuemei CHEN

Department of Electrical Engineering, Shaoyang University, Shaoyang 422000, China

Xiaoyu KANG, Fenghui ZHANG and Zhanwen HAN

Yunnan Observatory, Chinese Academy of Sciences, Kunming 650011, China

Key Laboratory for the Structure and Evolution of Celestial Objects, Chinese Academy of Sciences, Kunming 650011, China

(Received ; accepted)

Abstract

Tidally enhanced stellar wind may affect horizontal branch (HB) morphology in globular clusters (GCs) by enhancing the mass loss of primary star during binary evolution. Lei et al. (2013a, 2013b) studied the effect of this kind of wind on HB morphology in details, and their results indicated that binary is a possible second-parameter (2P) candidate in GCs. Binary fraction is an very important fact in the tidally-enhanced-stellar-wind model. In this paper, we studied the effect of binary fraction on HB morphology by removing the effects of metallicity and age. Five different binary fractions (i.e., 10%, 15%, 20%, 30% and 50%) are adopted in our model calculations. The synthetic HB morphologies with different binary fractions are obtained at different metallicities and ages. We found that, due to the great influence of metallicity and age, the effect of binary fraction on HB morphology may be masked by these two parameters. However, when the effects of metallicity and age are removed, the tendency that HB morphologies become bluer with increasing of binary fractions is clearly presented. Furthermore, we compared our results with the observation by Milone et al. (2012). Our results are consistent well with the observation at metal-rich and metal-poor GCs. For the GCs with intermediate metallicity, when the effect of age on HB morphology is removed, a weak tendency that HB morphologies become bluer with increasing of binary fractions is presented in all regions of GCs, which is consistent with our results obtained in this metallicity range.

Key words: stars: horizontal-branch - binaries: general - globular clusters: general

1. Introduction

The second parameter (2P) problem in globular clusters (GCs) is a puzzling problem which challenges our understanding on stellar evolution and formation history of GCs (see Catelan 2009 for a recent review). Most of the horizontal branch (HB) morphologies in GCs can be described by their different metallicities (Sandage & Wallerstein, 1960). However, more and more evidence from observations indicate that some other parameters, such as age, helium, binary, planet system, cluster mass, etc are also need as the second or third parameter affecting HB morphologies (Lee et al. 1994; Dotter et al. 2010; Gratton et al. 2010; D’Antona et al. 2002, 2005; D’Antona & Caloi 2004, 2008; Dalessandro et al. 2011, 2013; Valcarce, Catelan & Sweigart 2012; Lei et al. 2013a, 2013b; Soker 1998; Soker et al. 2000, 2001, 2007; Recio-Blanco et al. 2006). However, among these parameters, none of them can explain the whole HB morphologies in GCs successfully. Recently, the 2P problem is considered to be correlated with the multiple population phenomenon (Piotto et al. 2007; Gratton, Carretta & Bragaglia, 2012) and light elements anomalies found in GCs (e.g., Na-O, Mg-Al anti-correlation, Marino et al. 2011, 2014; also see Norris 1981; Norris et al. 1981; Kraft 1994), which makes this puzzling problem become more complicated.

Lei et al. (2013a, 2013b, hereafter Paper I and Paper II respectively, also see Han et al. 2012) proposed that tidally enhanced stellar wind during binary evolution may affect HB morphology by enhancing the mass loss of red giant primary star. In this scenario, the different mass loss for the progenitor of HB stars is caused by different separations of binary systems, and the number ratio of stars in different HB parts is affected by binary fractions used in the models (see the discussion in Paper II). These results indicate that binary populations may be the second or the third parameter candidate affecting HB morphologies in GCs. Sollima et al. (2007) and Milone et al. (2012) estimated the binary fraction of many Galactic GCs by analyzing the number of stars located on the red side of main-sequence (MS) fiducial line. They found low binary fraction in their GCs samples. Furthermore, Milone et al. (2012) found small or null relationship between binary fraction and HB morphology in their observation samples. However, they did not remove the effects of other important parameters when studying the effect of binary fraction on HB morphology, such as metallicity and age. Therefore, the motivation of this paper is to study the effect of binary fraction on HB morphology in details by considering the effects of metallicity and age under the tidally enhanced stellar wind.

The structure of this paper is as follows. In Section 2, we introduce the tidally-enhanced-stellar-wind model and code. The results and comparison with observation are given in Section 3. We discuss our results in Section 4. Finally a conclusion is given in Section 5.

2. Models and Code

The method used in this paper to obtain synthetic HB is the same as in Paper I and Paper II. Tidally enhanced stellar wind (Tout & Eggleton 1988) during binary evolution was incorporated into Eggleton’s stellar evolution code (Eggleton 1971, 1972, 1973; see Paper I and Paper II for details) to calculate the stellar mass and the helium core mass of the primary star at the helium flash (hereafter M_{HF} and $M_{\text{c,HF}}$, respectively). Then, M_{HF} , $M_{\text{c,HF}}$, and a time spent on HB were used to obtain the exact position of the primary star (e.g., effective temperature and luminosity) on HB in the Hertzsprung-Russell (H-R) diagram by interpolating among constructed HB evolutionary tracks. The time spent on HB in this paper means how long a HB star has been evolved from zero-age HB (ZAHB). Since the lifetime of HB stars is weakly dependent on the total mass when helium core mass is fixed, the time spent on HB is generated by a uniform random number between 0 and τ_{HB} (Rood 1973; Lee et al. 1990; Dalessandro et al. 2011). Here, τ_{HB} was set to be the lifetime of HB star with the lowest stellar mass among the constructed HB evolutionary tracks, which means that this star has the longest lifetime on the HB. All the HB evolutionary tracks were constructed using Modules for Experiments in Stellar Astrophysics (MESA; Paxton et al. 2011; see Paper I for details). Finally, we transform the effective temperature and luminosity of each HB star into $B - V$ colors and absolute magnitudes, M_V , using the Basel stellar spectra library (Lejeune et al. 1997, 1998) to obtain the synthetic HB morphology in color-magnitude diagram (CMD).

The parameters adopted in Eggleton’s stellar evolution code are the same as in Paper I and Paper II. The tidally enhanced stellar wind during binary evolution is described by the following equation,

$$\dot{M} = -\eta 4 \times 10^{-13} (RL/M) \{1 + B_w \times \min[(R/R_L)^6, 1/2^6]\}, \quad (1)$$

where η is the Reimers mass-loss efficiency (Reimers 1975); R_L is the radius of the Roche lobe; B_w is the tidal enhancement efficiency. R , L , M are the radius, luminosity and mass of the primary star in solar units.

We generate several groups of binary systems with different binary fractions. The initial orbital periods of all binary systems are produced by Monte Carlo simulations. The distribution of separation in binary is constant in $\log a$ (a is the separation) and falls off smoothly at small separations (Han et al. 2003),

$$a \cdot n(a) = \begin{cases} \alpha_{\text{sep}} (a/a_0)^m, & a \leq a_0, \\ \alpha_{\text{sep}}, & a_0 < a < a_1, \end{cases} \quad (2)$$

where $\alpha_{\text{sep}} \approx 0.07$, $a_0 = 10 R_{\odot}$, $a_1 = 5.75 \times 10^6 R_{\odot} = 0.13 \text{ pc}$ and $m \approx 1.2$. To study the effect of binary fraction on HB morphology, we adopt various value of binary fraction in model calculations (i.e., 10%, 15%, 20%, 30% and 50%)¹. The synthetic HB with different binary

¹ Note that these fractions are for the binary systems with their orbital periods less than 100 yr

Table 1. The input parameters for model calculations in this paper. The columns from left to right give metallicity, age of GCs and binary fraction respectively.

Z	age (Gyr)	f_{bin} (%)
0.02	10	10
		15
	12	20
		30
	13	50
0.001	10	10
		15
	12	20
		30
	13	50
0.0001	10	10
		15
	12	20
		30
	13	50

fractions are obtained at different metallicities and ages. The detailed input information for our model calculations in this paper is given in Table 1. The columns from left to right give metallicity, age of GCs and binary fraction, respectively. We use three different metallicities (e.g., $Z=0.02$, 0.001, 0.0001) in our model calculations, and for each metallicity, we adopt three different ages (e.g., 10, 12 and 13 Gyr). For each fixed metallicity and age, we adopt five different binary fractions (e.g., 10%, 15%, 20%, 30% and 50%).

3. Results

Fig.1 shows an example of synthetic HB morphology under tidally enhanced stellar wind for a binary fraction of 30%. In Fig.1, metallicity is $Z = 0.001$; age is 10 Gyr. HB stars located in RR Lyrae instability strip are denoted by crosses, and other HB stars are denoted by solid dots. The RR Lyrae instability strip is defined by the vertical region of $3.80 \leq \log T_{\text{eff}} \leq 3.875$ in the H-R diagram (Koopmann et al. 1994; Lee et al. 1990, see Fig.1 in Paper I). The label, $B : V : R$, is the number ratio of stars in different parts of HB, where B, V, R are the number of HB stars bluer than (or to the left of), within and redder than (or to the right of) the RR Lyrae instability strip (Lee et al. 1990). The label, HBR , is a parameter to describe HB morphology of GCs (Lee et al. 1994), and it is defined as follows,

$$HBR = (B - R)/(B + V + R), \quad (3)$$

where B, V, R have the same meaning as described above. The value of HBR is in the range of -1 to 1. The value of -1 means that all HB stars settle on red HB, while the value of 1 means

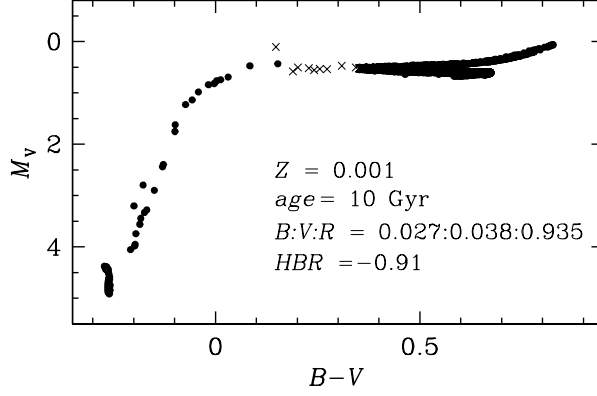


Fig. 1. An example of synthetic HB under tidally enhanced stellar wind for a binary fraction of 30%. HB stars located in RR Lyrae instability strip are denoted by crosses, and other HB stars are denoted by solid dots. B, V, R are the number of HB stars bluer than (or to the left of), within and redder than (or to the right of) the RR Lyrae instability strip. See the text for details.

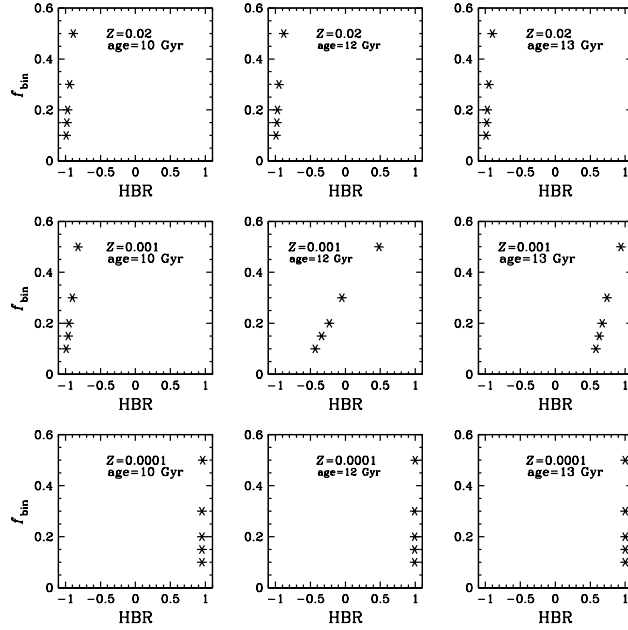


Fig. 2. Correlation between binary fraction and HB morphology under tidally enhanced stellar wind. The metallicity and age are fixed as labeled in each panel, but the binary fractions are different.

that GC presents a whole blue HB. Therefore, the larger of the HBR parameter, the bluer of HB morphology in GCs. For each synthetic HB morphology obtained in model calculation listed in Table 1, we obtain the value of HBR to study the correlation between binary fraction and HB morphology in GCs. The results are given in next section.

3.1. Effect of Binary Fraction on HB Morphology

Fig.2 shows the effect of binary fraction on HB morphology under tidally enhanced stellar wind. In each panel of Fig.2, the horizontal axis is the parameter HBR which is used to describe HB morphology, and the vertical axis is binary fraction. The synthetic GCs in each panel of Fig.2 have fixed metallicity and age but different binary fractions.

One can see that for the three top panels of Fig.2, in which synthetic GCs have a high metallicity of $Z=0.02$, though the binary fractions are different (e.g., from 10% to 50% in each panel), all synthetic GCs present a pure red HB morphology, and small or null effect of binary fraction on HB morphology is revealed. A similar result is also shown in the three bottom panels of Fig.2, in which GCs have a very low metallicity of $Z=0.0001$. All synthetic GCs in these three panels show a pure blue HB morphology regardless of the different binary fraction. This is due to the fact that metallicity influence HB morphology significantly at very high and very low metallicity, and it may mask the effect of binary fraction seriously.

However, for the three middle panels of Fig.2, in which synthetic GCs present an intermediate metallicity of $Z=0.001$, one can see that with the binary fraction increasing, the synthetic HB becomes bluer. This result is more clearly revealed especially in the middle panel in which synthetic GCs have an age of 12 Gyr (e.g., in this panel, with the binary fraction increasing from 10% to 50%, the value of HBR increases from about -0.5 to 0.5, which means the synthetic GCs transform from a dominant red HB to a blue HB). Nevertheless, the correlation between binary fraction and HB morphology is weakened in other two panels in which GCs have ages of 10 and 13Gyr. This result indicates that, age can also weaken the effect of binary fraction on HB morphology when GCs are very young or very old.

The results obtained from Fig.2 indicate that metallicity and age may mask the effect of binary fraction on HB morphology. However, for intermediate metallicity, when the effect of age is considered, our results reveal that higher binary fraction may make HB morphology become bluer. This is due to the fact that, in our scenario, when binary fraction increasing, more blue and extreme HB stars will be produced under tidally enhanced stellar wind (see the discussion in Paper II). In the next section, we will compare our results with recent observations.

3.2. Comparison with Observations

Milone et al. (2012) estimated the binary fraction for 59 Galactic GCs by analyzing the number of stars located on the red side of main-sequence fiducial line. Furthermore, they studied the relationship between binary fraction and HB morphology of GCs and found that there is a small or null effect of binary fraction on HB morphology. However, Milone et al.

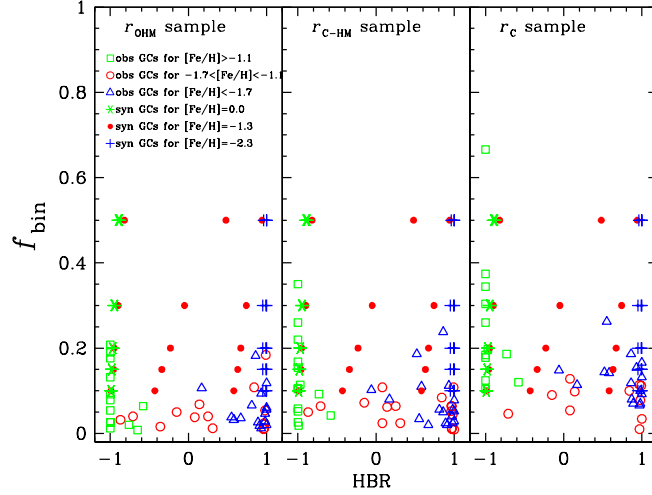


Fig. 3. Correlation between binary fraction and HB morphology for different regions of GCs. From left to right, these panels show the relationships from outside region to core region of the GCs (see the text for details). Green open squares, red open circles and blue open triangles denote observed GCs in metallicity range of $[\text{Fe}/\text{H}] > -1.1$, $-1.7 < [\text{Fe}/\text{H}] < -1.1$ and $[\text{Fe}/\text{H}] < -1.7$, respectively. The green asterisks, red solid circles and blue plus represent the synthetic GCs shown in Fig.2 at metallicity of $Z=0.02$, 0.001 , 0.0001 (or $[\text{Fe}/\text{H}]=0.0$, -1.3 , -2.3) respectively.

(2012) did not consider the effects of metallicity and age on HB morphology when studying the effect of binary fraction. As we have seen in Fig.2, these two parameters may mask the effect of binary fraction on HB morphology seriously.

In Fig.3, we compared our results obtained in Fig.2 with the observation by Milone et al. (2012). The binary fractions for observed GCs are from Milone et al. (2012), while metallicity, and HB morphology index, HBR , are from Carretta et al. (2010). The three panels represent three different regions of GCs which are defined by Milone et al. (2012). r_C means the region within one core radius of GC, and r_{C-HM} means the region between the core and the half-mass radius in GCs, while r_{OHM} means the region outside the half-mass radius in GCs. Therefore, the panels from left to right in Fig.3 show the relationship between binary fraction and on HB morphology from outside region to core region of GCs.

To weaken the effect of metallicity on HB morphology, we divide the observed GCs into three groups according to their metallicities. They are metal-rich group ($[\text{Fe}/\text{H}] > -1.1$, denoted by green open squares), intermediate metallicity group ($-1.7 < [\text{Fe}/\text{H}] < -1.1$, denoted by red open circles) and metal-poor group ($[\text{Fe}/\text{H}] < -1.7$, denoted by blue open triangles) respectively. In each panel, green asterisks, red solid circles and blue plus represent our synthetic GCs shown

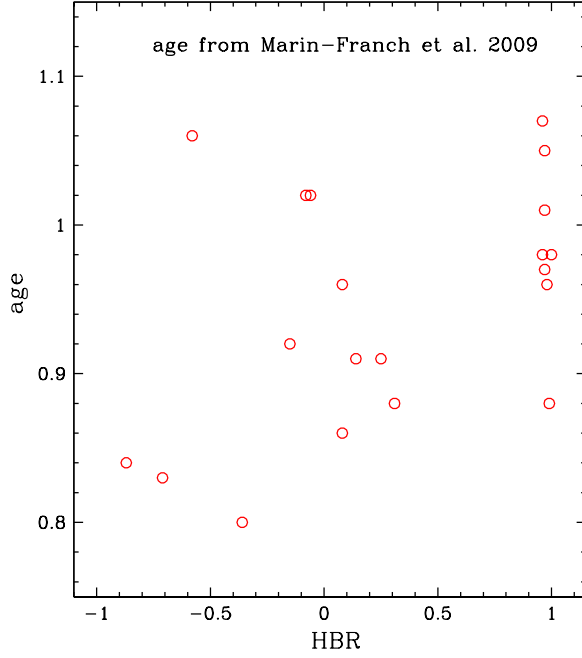


Fig. 4. Relationship between relative age and HB morphology for GCs in the intermediate metallicity group ($-1.7 < [\text{Fe}/\text{H}] < -1.1$).

in Fig.2 at metallicity of $Z=0.02$, 0.001 , 0.0001 (or $[\text{Fe}/\text{H}]=0.0$, -1.3 , -2.3), which correspond to metal-rich, intermediate metallicity and metal-poor group of observed GCs respectively (note that, for each metallicity we adopt three different ages, 10, 12, 13 Gyr, see Fig.2).

One can see clearly that in each panel of Fig.3, the observed GCs in metal-rich group show red HB morphologies, while observed GCs in metal-poor group present blue HB morphologies. We can not find any correlations between binary fraction and HB morphology for observed GCs in these two metallicity groups. This is due to the fact that metallicity (the first parameter) can significantly influence the HB morphology at very high and very low metallicity, and it masks the effect of binary fraction (even including the effect of age) on HB morphology. In these two metallicity groups, our synthetic GCs are consistent well with the observational data (see green asterisks and blue plus in each panel respectively). However, for the observed GCs in intermediate metallicity group, at first glance, there is still no evident correlation between binary fraction and HB morphology (see red open circles in each panel), which looks like to contradict with our results for this intermediate metallicity group. We will discuss this group of GCs in the next section in details.

4. Discussion

Though the effect of metallicity on HB morphology is weakened for observed GCs in the intermediate metallicity group, the age of GCs still can influence the HB morphology (Lee et

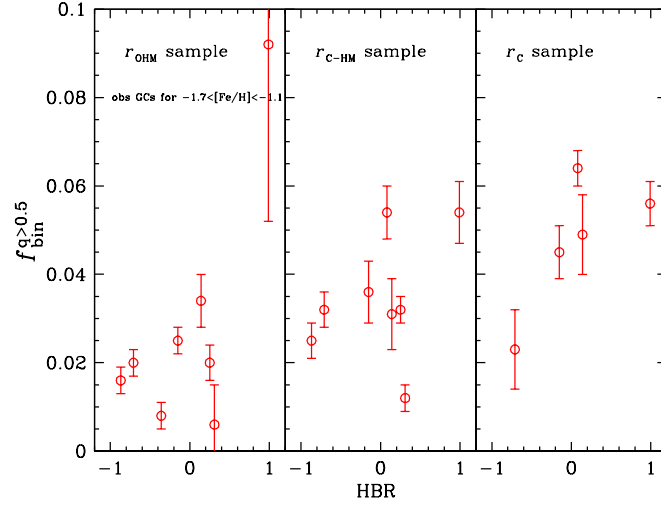


Fig. 5. Correlation between binary fraction and HB morphology for GCs in the intermediate metallicity group ($-1.7 < [\text{Fe}/\text{H}] < -1.1$), in which the oldest GCs are removed.

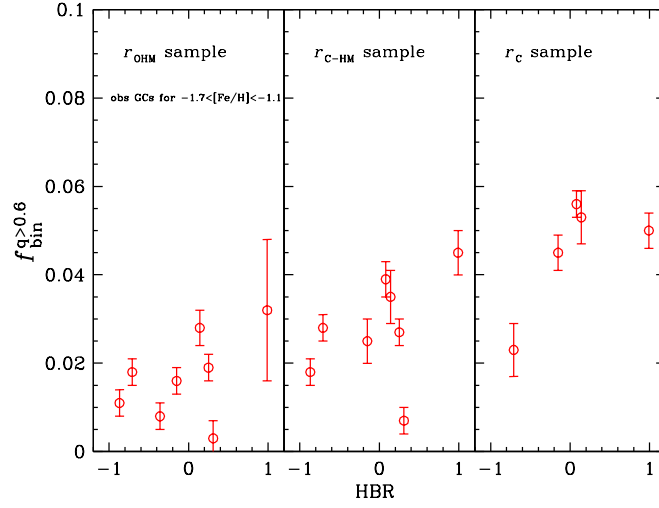


Fig. 6. Similar to Fig.5, but the binary fraction is for $q > 0.6$.

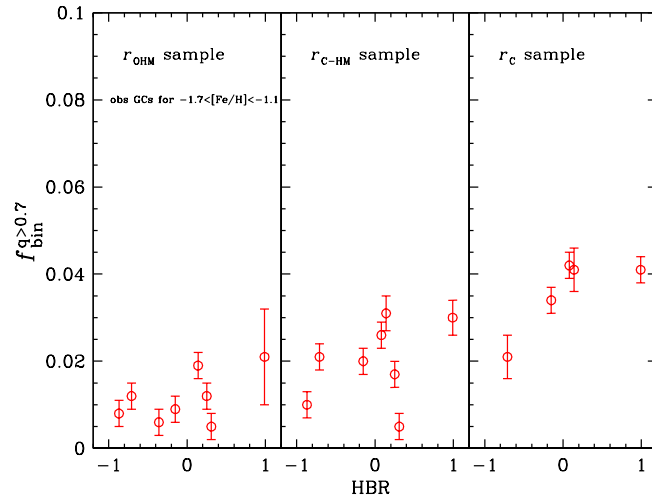


Fig. 7. Similar to Fig.5, but the binary fraction is for $q > 0.7$.

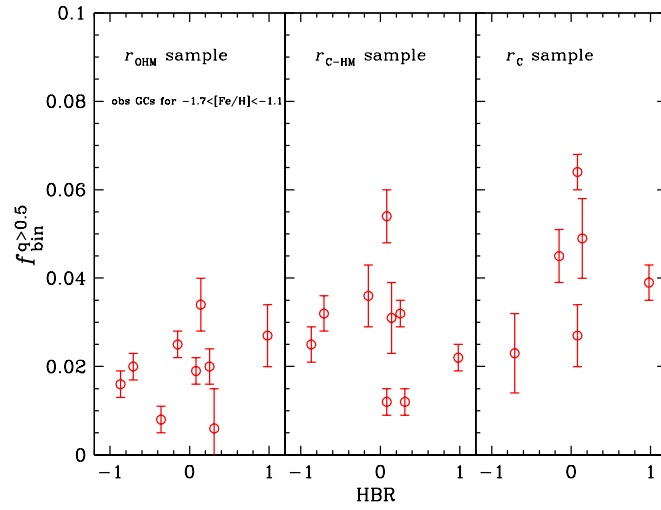


Fig. 8. Similar to Fig.5, but the age data of GCs is from De Angeli et al. (2005)

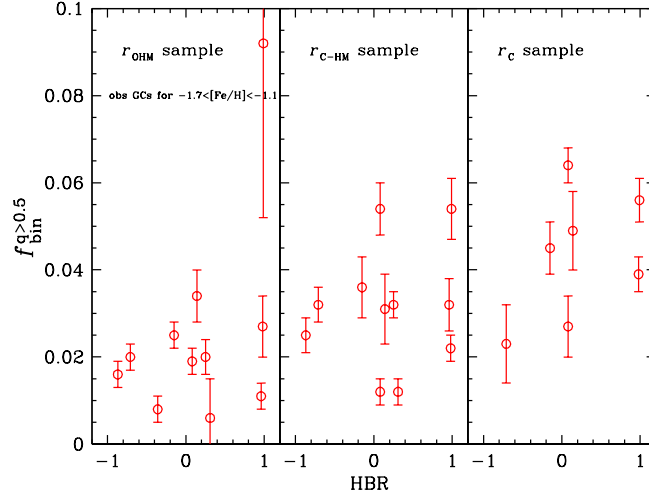


Fig. 9. Similar to Fig.5, but the age data of GCs is from VandenBerg et al. (2013)

al. 1994; Gratton et al. 2010; Dotter et al. 2010) , and it may also mask the effect of binary fraction as we discussed in Section 3.1. For this reason, we studied the age of the observed GCs distributed in the intermediate metallicity group. Fig.4 shows the relationship between relative age and HB morphology for observed GCs in the intermediate metallicity group ($-1.7 < [\text{Fe}/\text{H}] < -1.1$). The relative ages of the GCs are from Marin-Franch et al. (2009) which are defined as the ratio between cluster age and the mean age of the clusters in low-metallicity group. One can see clearly in Fig.4 that, the HB morphologies become bluer with increasing age of GCs. Especially for the oldest GCs (located in upper right of Fig.4), their HB morphologies are significantly affected by age, and they present nearly a pure blue HB (e.g., $HBR \simeq 1$).

To weaken the effect of age on HB morphology, We show in Fig.5 the relationship between binary fraction and HB morphology for observed GCs in the intermediate metallicity group by removing the oldest GCs (e.g., GCs with relative ages larger than about 0.96 in Fig.4 are removed). Note that, the total binary fraction of GCs in Milone et al. (2012) is obtained by assuming a constant mass-ratio distribution between 0 and 1 (see Section 5.2 in Milone et al. 2012). Under this assumption, it means that the binary fraction for $q > 0.5$ is equal to the binary fraction for $q < 0.5$, and the total binary fraction is simply 2 times of the binary fraction for $q > 0.5$. Therefore, the total binary fractions are dependent on the assumption of mass-ratio distribution. For this reason, the binary fraction used in Fig.5 is for $q > 0.5$, instead of the total binary fraction. One can see in Fig.5 that, though not very obviously, all the three panels present a weak correlation between binary fraction and HB morphologies, especially in the core region. With the binary fraction increasing, HB morphology becomes bluer.

We also study the effect of the binary fractions for $q > 0.6$ and 0.7 obtained in Milone et al. (2012) on HB morphology in the intermediate metallicity group of GCs ($-1.7 < [\text{Fe}/\text{H}] < -1.1$), and these binary fractions are independent on the assumption of mass-ratio distribution.

The results are given in Fig.6 and Fig.7. As in Fig.5, we also weaken the effect of age on HB morphology in these two figures by removing the oldest GCs (e.g., GCs with their relative ages larger than about 0.96 in Fig.4 are removed). One can see that the relationship between binary fraction and HB morphology present in Fig.6, 7 is very similar to the one in Fig.5. The relative ages of GCs used in Fig.4 are from Marin-Franch et al. (2009), and we also do the same analysis as in Fig.5, 6, 7 but using the age data from De Angeli et al. (2005) and VandenBerg et al. (2013) respectively. The results for $q > 0.5$ are shown in Fig.8 and 9, which are very similar to the one in Fig.5.

One may be aware of that the value of binary fractions adopted in our model calculations (i.e., 10%, 15%, 20%, 30% and 50%) are different from the ones obtained by Milone et al. (2012, most of them are less than 10%). Note that, the binary fractions in our model calculations are for the binary systems with their orbital periods less than 100 yr, but we do not know any information of orbital periods for the binary fraction obtained in Milone et al. (2012). Due to this reason, it is unlikely to directly use the binary fraction of a certain GC obtained by Milone et al. (2012) as input in our model calculations and then compare the results with the observation. However, the tendency that HB morphologies of GCs become bluer with increasing of binary fraction, though not very obviously in the observation², is consistent with our model calculation when the effects of metallicity and age are considered.

In a recent paper, Milone et al. (2014) defined two new parameters to describe the HB morphology, namely $L1$ and $L2$. They found that $L1$, which is the color difference between red giant branch (RGB) and HB in the CMD of GCs, correlates with cluster age and metallicity, while $L2$, which is the color extension of HB, correlates with the luminosity of GCs (M_V) and helium abundance. Milone et al. (2014) also found an anti-correlation between $L2$ and binary fraction in group 2 and group 3 GCs (see Fig.10 in their paper), which seems to demonstrate that a higher binary fraction corresponds to a shorter HB extension. This result does not contradict with our results obtained in this paper. One can see from Fig.3 in Milone et al. (2014) that more luminous (i.e. more massive) GCs present more extensional HB³, hence a longer $L2$. Meanwhile, more luminous (i.e. more massive) GCs also present lower binary fractions (see Fig.40 in Milone et al. 2012)⁴. These results reveal that the anti-correlation between $L2$ and binary fraction could be a result of the correlation between $L2$ and cluster

² This may be due to that binary is not the only second or third parameter affecting HB morphology (e.g., helium, cluster mass, etc may also at work in some GCs. Freeman & Norris 1981; Dotter et al. 2010; Gratton et al. 2010). In different GCs, the dominate second parameter may be different.

³ A possible explanation is that more massive GCs can retain the polluted material from the ejection of first-generation stars better than the less massive GCs (Recio-Blanco et al. 2006). These polluted material with higher helium abundance form the second-generation stars and extend the HB into bluer region (D’Antona et al. 2002).

⁴ A possible reason is that the mass of GCs and the binary destruction efficiency depend on the cluster density and velocity dispersion in a same way (Sollima 2008; Fregeau et al. 2009).

mass and the anti-correlation between binary fraction and cluster mass. Furthermore, the $L2$ parameter describes the extension of HB other than the specific number of HB stars in different HB regions. That is why $L2$ is sensitive to the L_t parameter (Fusi-Pecchi et al. 1993) and the maximum effective temperature of HB ($T_{\text{eff,Max}}$; Recio-Blanco et al. 2006), while insensitive to HBR parameter (see Fig.12 in Milone et al. 2014) which depends on the number ratio of HB stars located on different parts of HB. On the other hand, in our binary scenario, different binary fractions would alter the number of HB stars in different HB regions (see Paper I and Paper II for details), hence it correlates with HBR parameter.

5. Conclusion

In this paper, we studied the effect of binary fraction on HB morphology under tidally enhanced stellar wind. We adopted five different binary fractions, i.e., 10%, 15%, 20%, 30% and 50%, in our model calculations. Our results revealed that for the GCs with intermediate metallicity and age, the correlation between binary fraction and HB morphology is clear. With binary fractions increasing, HB morphologies become bluer. However, metallicity and age may mask the effect of binary fraction on HB morphology. We also compared our results with the observation of Milone et al. (2012). We found that our results are consistent well with the observed GCs in metal-rich and metal-poor group. Moreover, when the effect of age on HB morphology for the intermediate metallicity group of GCs is removed, a weak correlation between binary fraction and HB morphology is presented in all regions of GCs, and the tendency that HB morphology becomes bluer with increasing of binary fractions is consistent with our results.

This work is supported by the Key Laboratory for the Structure and Evolution of Celestial Objects, Chinese Academy of Science (OP201302).

References

- Carretta, E., Bragaglia, A., Gratton, R. G.; et al. 2010, A&A, 516, A55
- Catelan, M. 2009, Ap&SS, 320, 261
- Dalessandro, E., Salaris, M., Ferraro, F. R., et al. 2011, MNRAS, 410, 694
- Dalessandro, E., Salaris, M., Ferraro, F. R., Mucciarelli, A., Cassisi, S., 2013, MNRAS, 430, 459
- D’Antona, F., Bellazzini, M., Caloi, V., Fusi Pecci, F., Galletti, S., & Rood, R. T. 2005, ApJ, 631, 868
- D’Antona, F., & Caloi, V. 2004, ApJ, 611, 871
- D’Antona, F., & Caloi, V. 2008, MNRAS, 390, 693
- D’Antona, F., Caloi, V., Montalbán, J., Ventura, P., & Gratton, R. 2002, A&A, 395, 69
- De Angeli, F., Piotto, G., Cassisi, S. et al. 2005, AJ, 130, 116
- Dotter, A., Sarajedini, A., Anderson, J., et al. 2010, ApJ, 708, 698
- Eggleton, P. P. 1971, MNRAS, 151, 351

- Eggleton, P. P. 1972, MNRAS, 156, 361
- Eggleton, P. P. 1973, MNRAS, 163, 279
- Freeman, K. C. & Norris, J. 1981, ARA&A, 19, 319
- Fregeau, J. M., Ivanova, N., & Rasio, F. A. 2009, ApJ, 707, 1533
- Fusi Pecci, F., Ferraro, F. R., Bellazzini, M., Djorgovski, S., Piotto, G., & Buonanno, R. 1993, AJ, 105, 1145
- Gratton, R. G., Carretta, E., & Bragaglia, A., 2012, A&A Rev., 20, 50
- Gratton, R. G., Carretta, E., Bragaglia, A., et al. 2010, A&A, 517, A81
- Han, Z., Chen, X., Lei, Z., & Podsiadlowski, P. 2012, ASPC, 452, 3
- Han, Z., Podsiadlowski, Ph., Maxted, P. F. L., & Marsh, T. R. 2003, MNRAS, 341, 669
- Koopmann, R. A., Lee, Y. W., Demarque, P., et al. 1994, ApJ, 423, 380
- Kraft, R. P., 1994, PASP, 106, 553
- Lee, Y. W., Demarque, P., & Zinn, R. 1990, ApJ, 350, 155
- Lee, Y. W., Demarque, P., & Zinn, R. 1994, ApJ, 423, 248
- Lei, Z., Chen, X., Zhang, F., & Han, Z. 2013a, A&A, 549, A145, Paper I
- Lei, Z., Zhang, F., Ge, H., & Han, Z. 2013b, A&A, 554, A130, Paper II
- Lejeune, T., Cuisinier, F., & Buser R. 1997, A&AS, 125, 229
- Lejeune, T., Cuisinier, F., & Buser R. 1998, A&AS, 130, 65
- Marin-Franch, A., Aparicio, A., & Piotto, G., et al. 2009, ApJ, 694, 1498
- Marino, A. F., Milone, A. P., Przybilla, N., et al. 2014, MNRAS, 437, 1609
- Marino, A. F., Villanova, S., Milone, A. P., et al. 2011, ApJ, 730, L16
- Milone, A. P., Marino, A. F., Dotter, A., et al. 2014, ApJ, 785, 21
- Milone, A. P., Piotto, G., Bedin, L. R., et al. 2012, A&A, 540, A16
- Norris, J. 1981, ApJ, 248, 177
- Norris, J., Cottrell, P. L.; Freeman, K. C.; Da Costa, G. S. ApJ, 1981, 244, 205
- Paxton, B., Bildsten, L., Dotter, A., et al. 2011, ApJS, 192, 3
- Piotto, G., Bedin, L. R., Anderson, J., et al. 2007, ApJ, 661, L53
- Recio-Blanco, A., Aparicio, A., Piotto, G., De Angeli, F., & Djorgovski, s. G. 2006, A&A, 452, 875
- Reimers, D. 1975, MSRSL, 8, 369
- Rood, R. T. 1973, ApJ, 184, 815
- Sandage, A., & Wallerstein, G. 1960, ApJ, 131, 598
- Soker, N. 1998, AJ, 116, 1308
- Soker, N., & Hadar, R. 2001, MNRAS, 324, 213
- Soker, N., & Harpaz, A. 2000, MNRAS, 317, 861
- Soker, N., & Harpaz, A. 2007, ApJ, 660, 699
- Sollima, A. 2008, MNRAS, 388, 307
- Sollima, A., Beccari, G., Ferraro, F. R., et al. 2007, MNRAS, 380, 781
- Tout, C. A., & Eggleton, P. P. 1988, MNRAS, 231, 823
- Valcarce, A. A. R., Catelan, M., & Sweigart, A. V., 2012, A&A, 547, A5
- VandenBerg, Don A.; Brogaard, K.; Leaman, R.; Casagrande, L. 2013, ApJ, 775, 134